VOL.101 NO.GT9. SEPT. 1975

JOURNAL OF THE GEOTECHNICAL ENGINEERING DIVISION

PROCEEDINGS OF
THE AMERICAN SOCIETY
OF CIVIL ENGINEERS

CONTENTS

→

This Journal is published monthly by the American Society of Civil Engineers. Publications office is at 345 East 47th Street, New York, N.Y. 10017. Address all ASCE correspondence to the Editorial and General Offices at 345 East 47th Street, New York, N.Y. 10017. Allow six weeks for change of address to become effective. Subscription price to members is $10.00. Nonmember subscriptions available; prices obtainable on request. Second-class postage paid at New York, N.Y. and at additional mailing offices. HY, GT.

DISCUSSION

Proc. Paper 11534

TECHNICAL NOTES

Proc. Paper 11538

[a]Discussion period closed for this paper. Any other discussion received during this discussion period will be published in subsequent Journals.

INFORMATION RETRIEVAL

The key words, abstract, and reference "cards" for each article in this Journal represent part of the ASCE participation in the EJC information retrieval plan. The retrieval data are placed herein so that each can be cut out, placed on a 3 × 5 card and given an accession number for the user's file. The accession number is then entered on key word cards so that the user can subsequently match key words to choose the articles he wishes. Details of this program were given in an August, 1962 article in CIVIL ENGINEERING, reprints of which are available on request to ASCE headquarters.

JOURNAL OF THE GEOTECHNICAL ENGINEERING DIVISION

STABILITY OF EMBANKMENT ON CLAY

By Tien H. Wu,[1] F. ASCE, William B. Thayer,[2] A. M. ASCE, and Sheng S. Lin[3]

INTRODUCTION

In 1969, the Ohio Department of Transportation began construction of the interchange for Interstate Routes 77 and 80 at Independence, Ohio. The project included a high embankment and a deep excavation as shown in Fig. 1. The embankment was almost completed to the final height in March 1971 when a slide occurred. The extent of the slide is also shown in Fig. 1.

This paper summarizes the construction performance of the embankment, followed by a description of the detailed investigation carried out to determine the mechanism of the slide.

GEOLOGY AND SUBSOIL CONDITIONS

The site was located in the Cuyahoga River Valley about 5 miles (8.1 km) south of Cleveland. During the Illinoian and Wisconsin glaciation the valley was repeatedly covered by the continental glaciers and related glacial lakes of various levels. The glacial geology and history of the lakes have been described by Leverett (3). According to Leverett's map the site was submerged under the water of Lake Maumee. Studies by Bagley (1) have revealed that the subsoil in the Cuyahoga Valley is comprised of four till layers separated by lacustrine clays, which indicate the presence of glacial lakes older than Lake Maumee.

The subsoil conditions at the site are shown in Figs. 2, 3, and 4. In general, a thick layer of lacustrine clay extends from the surface to about El. 605 ft (184 m). The major portion of this consists of varved clay which is a silty clay with silt and fine sand laminations. Shear displacements in the varves have been observed in several samples [Fig. 5(*a*)]. Within this lacustrine clay

Note.—Discussion open until February 1, 1976. To extend the closing date one month, a written request must be filed with the Editor of Technical Publications, ASCE. This paper is part of the copyrighted Journal of the Geotechnical Engineering Division, Proceedings of the American Society of Civil Engineers, Vol. 101, No. GT9, September, 1975. Manuscript was submitted for review for possible publication on May 29, 1974.

[1]Prof. of Civ. Engrg., Ohio State Univ., Columbus, Ohio.
[2]Engr., E. D'Appolonia Consulting Engrs., Pittsburgh, Pa.
[3]Grad. Research Assoc., Ohio State Univ., Columbus, Ohio.

and between El. 605 ft and 630 ft (184 m and 192 m) are layers containing different proportions of silt and clay. The "silt" layers contain up to 70% silt, whereas the "clay" layers contain about 50% silt; the remainder consists mostly of particles smaller than 2μ. The liquid and plastic limits are around 29% and 17% for the "silt" layers and around 40% and 15% for the "clay" layers. The thickness of the individual layers range from about 1 in.-24 in. (25 mm-610 mm); the thicker layers are mostly "clay." In Figs. 2, 3, and 4 the individual "silt" and "clay" layers are not identified and are shown together as silty clay. The strength of the "clay" is variable and ranges from soft to medium. Slickensides [Fig. 5(*b*)] have been found in several samples, some of which were taken before the slide occurred. The major portion of the failure surface at Section AA passed through the soft clay layer near El. 612 ft (187 m). Note that the ground surface at Section CC is near El. 600

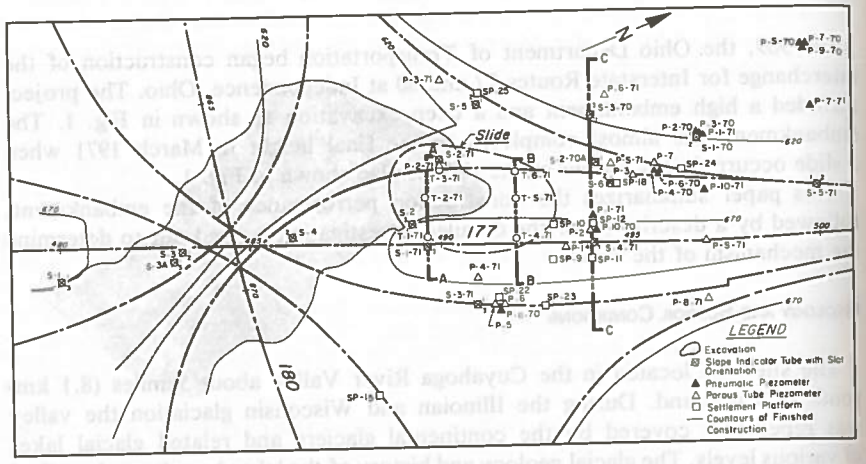

FIG. 1.—Location Plan (Station Numbers Are in 100 ft; Contour Elevations Are in feet) (1 ft = 0.305 m)

ft (180 m). Thus, the material described in this paragraph is not present in this section.

Below approx El. 605 ft (184 m) there is a layer of glacial till whose base is located between El. 570 ft and 580 ft (174 m and 177 m). A second layer of varved clay exists below this till. Its character is similar to the first varved clay layer. Within the second varved clay a layer of soft to medium silty clay up to 5 ft (1.5 m) thick has been encountered in some borings. Its liquid and plastic limits are around 40% and 20%, respectively. Slickensides have also been found in this clay. The potential failure surface at Section CC passed through this layer. Below El. 540 ft (165 m) lies another layer of till. The stiffness of the till increases with depth and standard penetration resistances of 50 blows/ft (160 blows/m) or more have been recorded near El. 510 ft (156 m).

Bedrock was encountered at El. 540 ft (165 m) in a boring 900 ft (280 m)

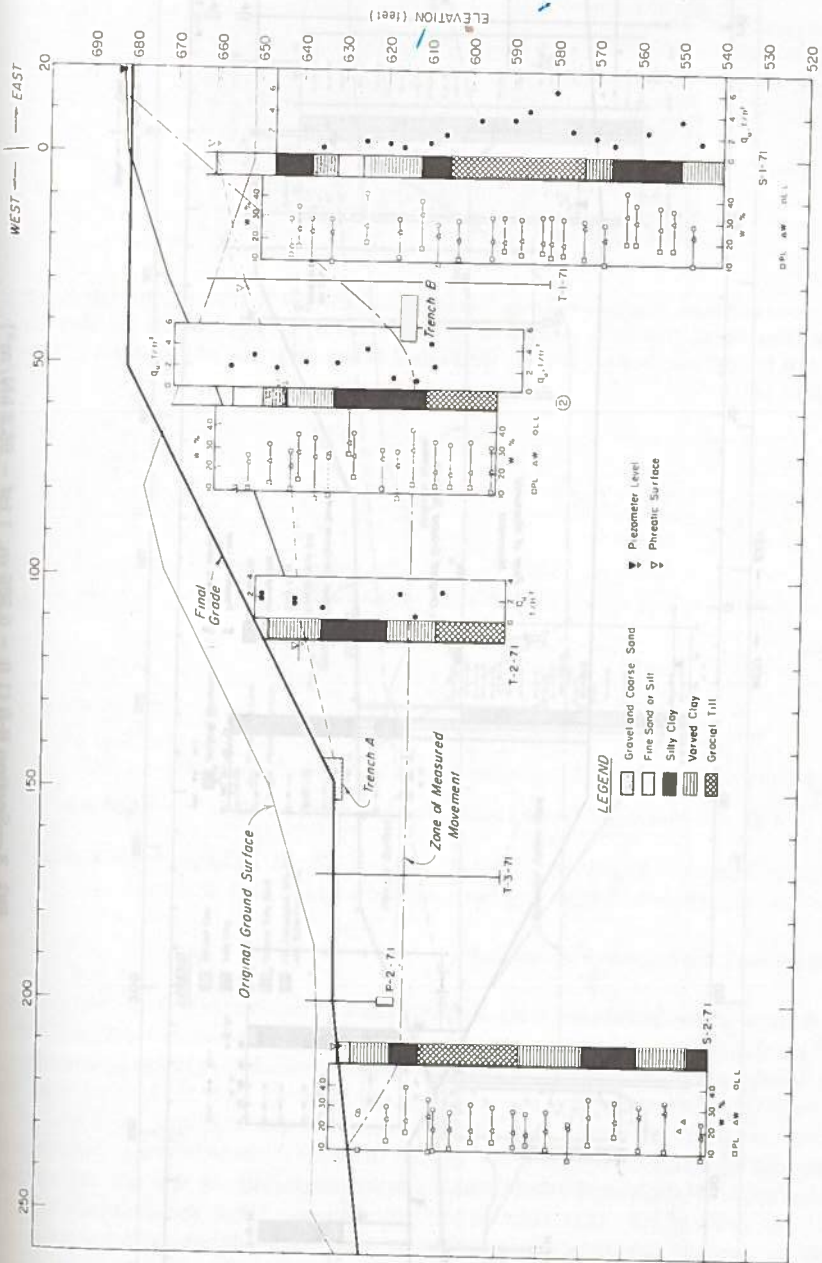

FIG. 2.—Section A-A (1 ft = 0.305 m; 1 tsf = 95.8 kN/m²)

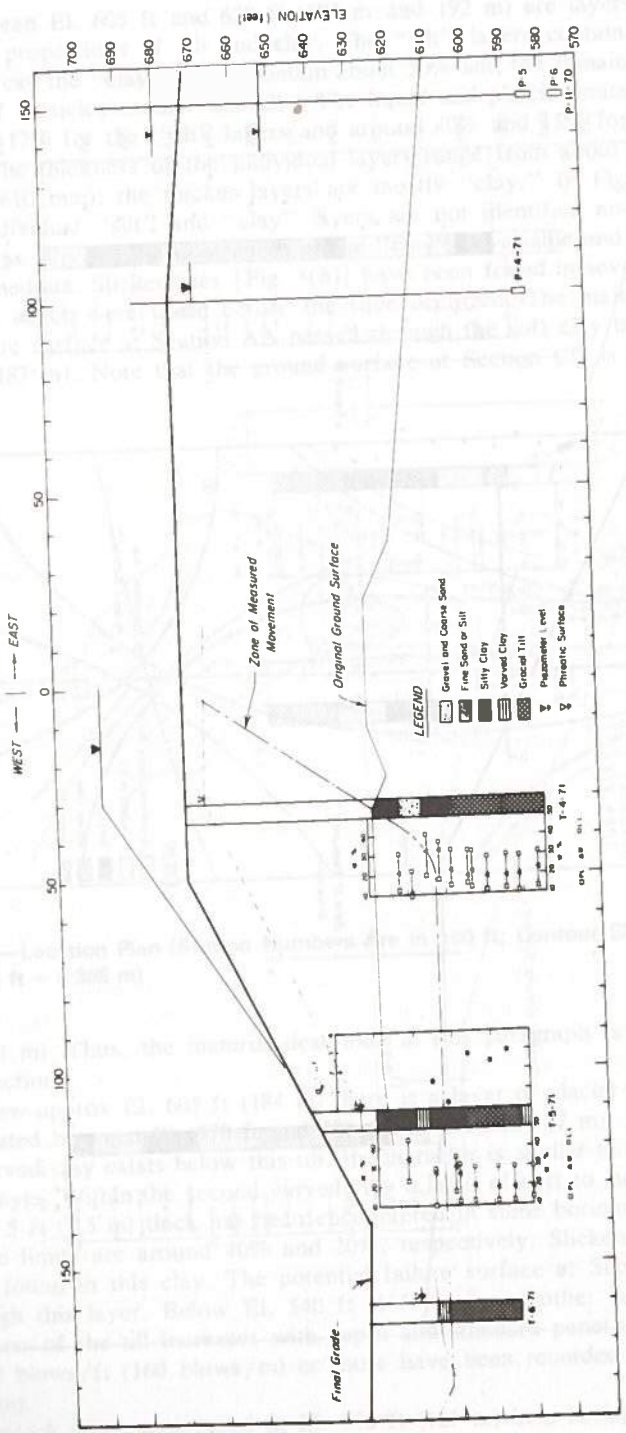

FIG. 3.—Section B-B (1 ft = 0.305 m; 1 tsf = 95.8 kN/m²)

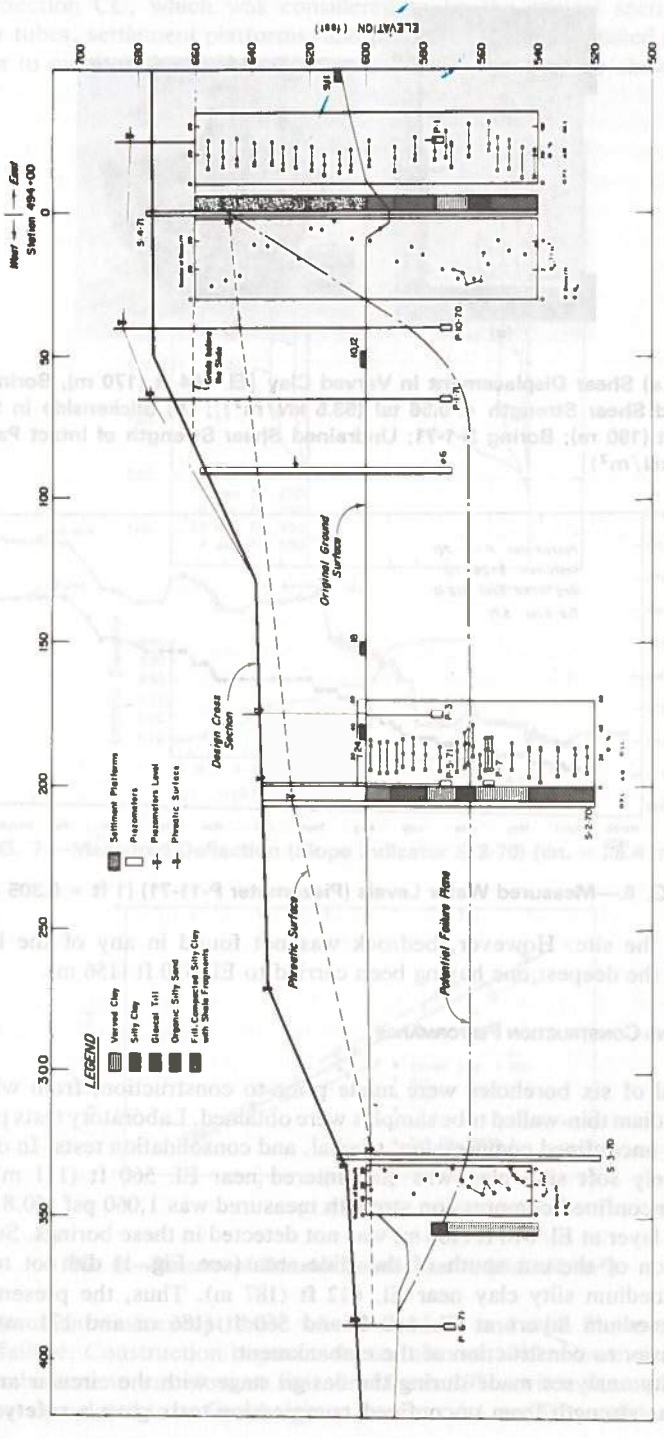

FIG. 4.—Section C-C (1 ft = 0.305 m; 1 tsf = 95.8 kN/m²)

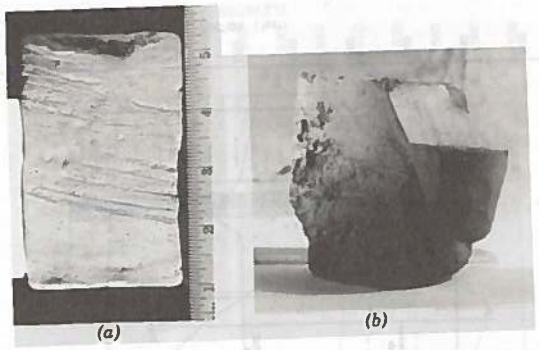

FIG. 5.—(a) Shear Displacement in Varved Clay [El. 564 ft (170 m), Boring S-4-71; Undrained Shear Strength = 0.56 tsf (53.5 kN/m²)]; (b) Slickenside in Silty Clay [El. 628 ft (190 m); Boring S-1-71; Undrained Shear Strength of Intact Part = 0.44 tsf (42.1 kN/m²)]

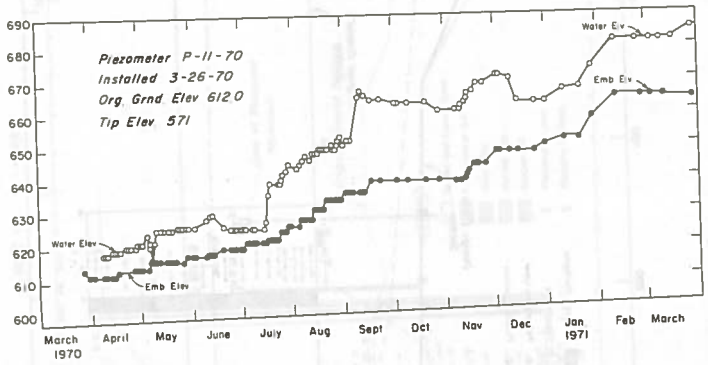

FIG. 6.—Measured Water Levels (Piezometer P-11-71) (1 ft = 0.305 m)

west of the site. However, bedrock was not found in any of the borings at the site, the deepest one having been carried to El. 510 ft (156 m).

Design and Construction Performance

A total of six boreholes were made prior to construction, from which 3-in. (76-mm) diam thin-walled tube samples were obtained. Laboratory tests performed included unconfined compression, triaxial, and consolidation tests. In one boring a relatively soft silty clay was encountered near El. 560 ft (171 m) and the lowest unconfined compression strength measured was 1,060 psf (50.8 kN/m²). The soft layer at El. 610 ft (186 m) was not detected in these borings. Subsequent excavation of the cut south of the slide area (see Fig. 1) did not reveal any soft to medium silty clay near El. 612 ft (187 m). Thus, the presence of the soft to medium layers at El. 610 ft and 560 ft (186 m and 171 m) was not known prior to construction of the embankment.

Stability analyses made during the design stage with the circular arc method and shear strength from unconfined compression tests gave a safety factor of

2.2 for Section CC, which was considered to be the critical section. Slope indicator tubes, settlement platforms, and piezometers were installed at various locations to monitor the field performance. Their locations are shown in Fig.

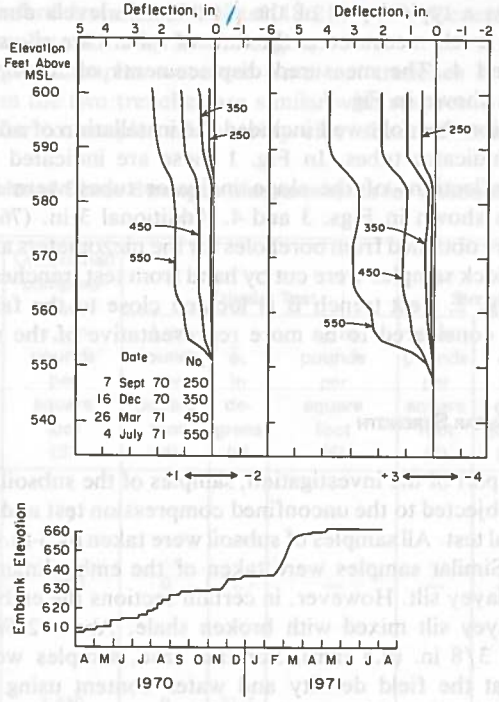

FIG. 7.—Measured Deflection (Slope Indicator S-3-70) (lin. = 25.4 mm)

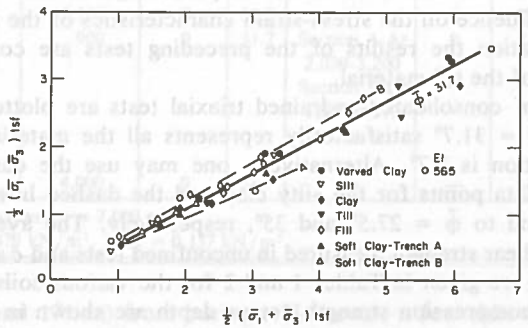

FIG. 8.—Results of Triaxial Tests (1 tsf = 95.8 kN/m²)

1. All instrumentation except those whose numbers end with 71 were installed prior to failure. Construction began in the autumn of 1969. However, progress on the embankment was slow at first. In March 1971, when the embankment was almost completed to its final height at Sections AA and BB, a slide occurred.

The extent of the slide was clearly identifiable by cracks at the top of the embankment and bulges near the toe. Subsequently large horizontal movements were recorded by the slope indicator measurements at Section CC and construction was stopped in this section with the top of the embankment at El. 660 ft (201 m). Fig. 6 shows a typical plot of the piezometric levels during construction. The piezometric levels measured at the time of failure are shown on the sections in Figs 2, 3, and 4. The measured displacements of a slope indicator tube at Section CC is shown in Fig. 7.

The investigation that followed included the installation of additional piezometers and slope indicator tubes. In Fig. 1 these are indicated by numbers that end with 71. Deflections of the slope indicator tubes were used to establish the slip surfaces shown in Figs. 3 and 4. Additional 3 in. (76-mm) thin-walled tube samples were obtained from boreholes for the piezometers and slope indicator tubes. Several block samples were cut by hand from test trenches whose locations are shown in Fig. 2. Test trench B is located close to the failure surface and the samples are considered to be more representative of the soil in the failure zone.

Investigation of Shear Strength

General.—As part of the investigation, samples of the subsoil and embankment material were subjected to the unconfined compression test and the consolidated-undrained triaxial test. All samples of subsoil were taken by 3-in. (76-mm) thin-wall tube samplers. Similar samples were taken of the embankment material where it consisted of clayey silt. However, in certain sections the embankment material consisted of clayey silt mixed with broken shale. About 25% of this material was larger than 3/8 in. (9.5 mm). For this case, samples were compacted in the laboratory at the field density and water content using the soil fraction that passed the 3/8-in. (9.5-mm) sieve. The measured strengths are close to those of the tube samples. Hirst and Mitchell (5) have shown that if a sand-clay mixture contains less than 50% sand, the percentage of sand does not exert a significant influence on the stress-strain characteristics of the mixture. Based on this observation the results of the preceding tests are considered to be representative of the fill material.

The results of consolidated-undrained triaxial tests are plotted in Fig. 8. It appears that $\bar{\phi} = 31.7°$ satisfactorily represents all the materials tested. The standard deviation is 2.7°. Alternatively, one may use the dashed line A to represent the data points for the silty clay and the dashed line B for the fill. They correspond to $\bar{\phi} = 27.5°$ and 35°, respectively. The average values of the undrained shear strength measured in unconfined tests and $\bar{c}$ and $\bar{\phi}$ measured in triaxial tests are given in Tables 1 and 2 for the various soils. Typical plots of unconfined compression strength versus depth are shown in Figs. 2, 3, and 4. The soft silty clays at El. 610 ft and 560 ft (186 m and 171 m) coincide with the horizontal portions of the slip surfaces in Sections AA and CC, respectively.

Shear Strength of Silty Clay.—Since large portions of the slip surfaces in both sections passed through silty clay the strength properties of the soft soils near El. 612 ft and 565 ft (187 m and 172 m) were subjected to detailed investigation.

While all borings in the slide area and near Section CC encountered the

silty clay the strength varies considerably from one locality to another. A total of 16 unconfined compression tests were made on tube samples obtained near El. 612 ft and 565 ft (187 m and 172 m). The undrained shear strength ranges from 0.15 tsf–0.68 tsf (14.4 kN/m²–65 kN/m²) with a mean of 0.45 tsf (43 kN/m²) and a standard deviation of 0.19 tsf (18.2 kN/m²). Generally, slickensides were found in samples with very low strengths.

A number of block samples were cut from test trenches A and B (Fig. 2). The materials from the two trenches are similar with respect to Atterberg limits and are also similar to samples of the silty clay obtained near El. 612 ft and

TABLE 1.—Results of Shear Strength Measurements for Sections A-A and B-B

Soil type (1)	Bulk density, in pounds per cubic foot (2)	Unconfined compression, s_u, in pounds per square foot (3)	Triaxial Test			Simple Shear Test		
			$\bar{c}$, in pounds per square foot (4)	$\bar{\phi}$, in degrees (5)	s_u, in pounds per square foot (6)	$\bar{c}$, in pounds per square foot (7)	$\bar{\phi}$, in degrees (8)	s_u, in pounds per square foot (9)
Fill-gray clay and shale fragments	140	800	0	31.7	—	—	—	—
Brown silty clay and varved clay El. 630–660	125	1,650	0	31.7	—	—	—	—
Uniform gray clay El. 623–630	125	1,200	0	31.7	—	0	22	—
Gray silty clay El. 610–623	125	900	0	31.7	Section A-A[a] 2,030–3,200 Section B-B[a] 1,270–1,370	0	22	Section A-A[a] 645–1,180 Section B-B[a] 440
Glacial till below El. 610	125	4,000	0	31.7	—	—	—	—

[a]Preconsolidation pressure = 7,000 psf.
Note: 1 psf = 0.0479 kN/m²; 1 pcf = 0.157 kN/m³.

565 ft (186 m and 171 m) from borings. However, a few thin silt layers were found in the block samples from trench B and none in those from trench A. Unconfined compression and unconsolidated undrained triaxial tests performed on nine samples trimmed from the blocks gave undrained shear strengths from 0.45 tsf–0.64 tsf (43 kN/m²–61 kN/m²) with a mean of 0.54 tsf (51.7 kN/m²) and sensitivities from 1.5–2.3. Thus, the average strength is considerably higher than that of the tube samples. One may question the effect of sampling disturbance on strength. While the strengths of many tube samples are smaller than the

previous values, their sensitivities are also between 1.5 and 2. However, this information is not sufficient for determination of the sample disturbance.

To study the effect of stress state on shear strength, a series of consolidated-undrained simple shear tests (2) was performed on samples from the test trenches. In series 1, the samples were consolidated under different vertical stresses smaller than the preconsolidation pressure and then sheared at constant volume. In series 2 the samples were first consolidated under 6.0 tsf (575 kN/m^2) and then allowed to swell under reduced stresses. After this they were sheared at constant volume. The volume was maintained constant by continuous adjustment of the vertical stress during shear.

Ladd (6,7,8) has used the relationship between normalized shear strength $s_u/\bar{\sigma}_{vc}$ and overconsolidation ratio OCR to evaluate the in-situ shear strength, in which $\bar{\sigma}_{vc}$ denotes the vertical stress. In series 1, the maximum vertical stress, $\bar{\sigma}_{vm}$, is equal to the preconsolidation pressure, p, of the clay deposit;

TABLE 2.—Results of Shear Strength Measurements for Section C-C

Soil type (1)	Bulk density, in pounds per cubic foot (2)	Unconfined compression, s_u, in pounds per square foot (3)	Triexiel Test			Simple Sheer Test		
			$\bar{c}$, in pounds per square foot (4)	$\bar{\phi}$, in degrees (5)	s_u, in pounds per square foot (6)	$\bar{c}$, in pounds per square foot (7)	$\bar{\phi}$, in degrees (8)	s_u, in pounds per square foot (9)
Fill-gray clay and shale fragments	140	800	0	31.7	—	—	—	—
Gray and brown organic silt	125	1,200	0	31.7	—	—	—	—
Glacial till El. 575-590	125	4,000	0	31.7	—	—	—	—
Varved clay El. 565-575	125	2,000	0	31.7	—	—	—	—
Gray silty clay El. 555-565	125	900	0	31.7	2,500[a]	0	22	1,190[a]

[a]Preconsolidation pressure = 7,000 psf.
Note: 1 psf = 0.0479 kN/m^2; 1 pcf = 0.157 kN/m^3.

this is equal to 2.5 tsf (239 kN/m^2) for samples from trench A and about 3.5 tsf (335 kN/m^2) for samples from trench B according to the e-log p curves obtained from consolidation tests. In series 2, the value of $\bar{\sigma}_{vm}$ is 6 tsf (575 kN/m^2). The test results are shown in Fig. 9(a). The data for trench A indicate that the results from series 1 and 2 are not very different. In view of the significant difference between the strengths of the samples from the two trenches, we note that several of the samples from trench B contained slickensides and fissures. Their direction was nearly horizontal.

The shear strength along the failure surface was obtained by multiplying the value of $s_u/\bar{\sigma}_{vc}$ for the appropriate OCR by the existing overburden pressure. For simple shear, the results of samples from trench B were used in the calculations. The calculated values are given in Tables 1 and 2. The shear strength

varies because of variations in the initial overburden pressure across the section. The results of the simple shear tests were also used to determine values of $\bar{c}$ and $\bar{\phi}$. For the condition of maximum shear stress, the value of $\bar{\phi}$ is about

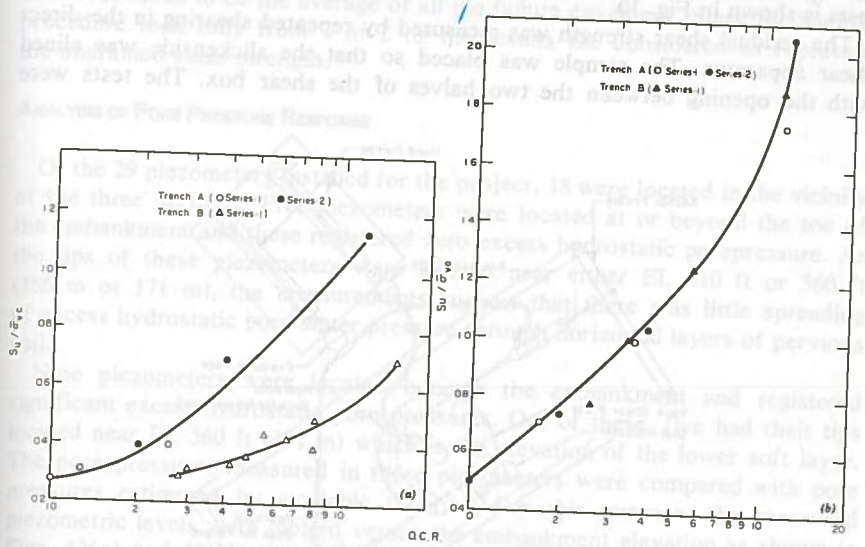

FIG. 9.—Normalized Shear Strength: (*a*) Simple Shear Test; (*b*) Triaxial Test

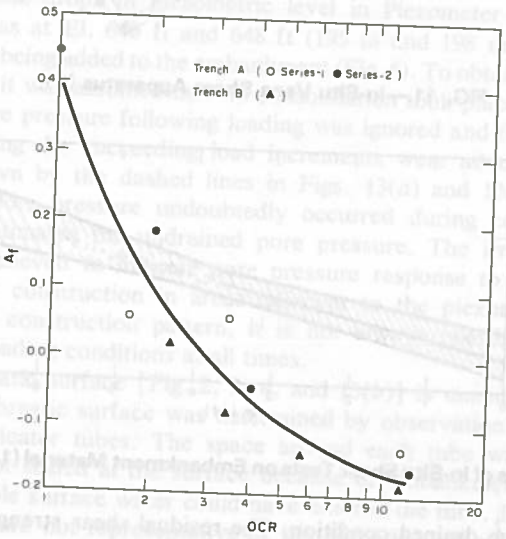

FIG. 10.—Pore Pressure Parameter A Versus Overconsolidation Ratio

22°. This value is also given in Tables 1 and 2.

For comparison, consolidated-undrained triaxial tests were also performed. The samples were consolidated isotropically and then sheared in the undrained

condition. The stresses used for consolidation followed the same pattern as those used in the simple shear tests. The results are shown in Fig. 9(*b*). The influence of the OCR on the pore pressure parameter, *A*, measured in triaxial tests is shown in Fig. 10.

The residual shear strength was measured by repeated shearing in the direct shear apparatus. The sample was placed so that the slickenside was alined with the opening between the two halves of the shear box. The tests were

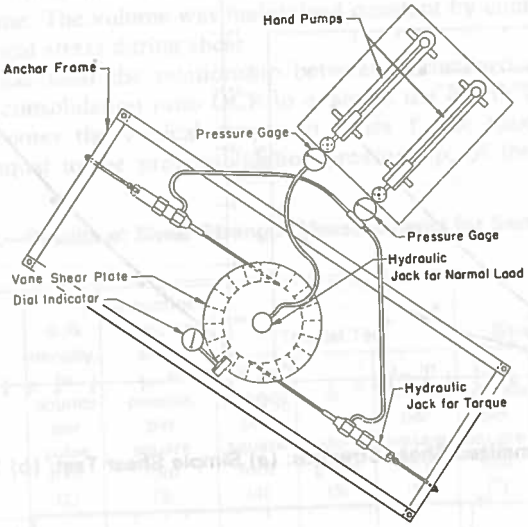

FIG. 11.—In-Situ Vane Shear Apparatus (11)

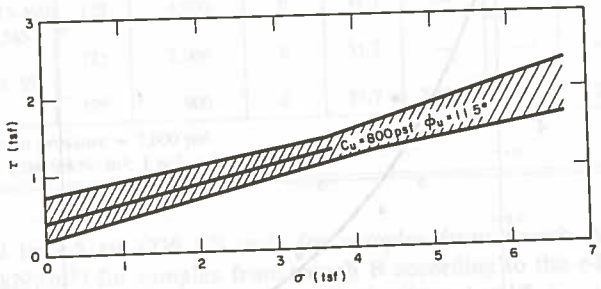

FIG. 12.—Results of In-Situ Shear Tests on Embankment Material (1 tsf = 95.8 kN/m²)

performed in the drained condition. The residual shear strength is represented by $\bar{\phi}_r = 14°$.

In-Situ Shear Tests.—During the repair of the slide several in-situ vane shear tests were performed on the fill material (9). A schematic diagram of the apparatus is shown in Fig. 11. The vane shear plate has a 12-in. (300-mm) OD and an 8-in. (200-mm) ID. A normal force was applied to the vane shear plate and the shear force was applied by a torque which was increased until failure occurred.

After this the normal stress was increased and the process repeated. The range in the normal stress is from 0.67 tsf–6.00 tsf (64 kN/m²–580 kN/m²). The normal and shear stresses at failure fall within the shaded zone in Fig. 12. Line A is taken to be the average of all the failure envelopes. Since the loading procedure took only from 1 hr–2 hr the results are considered to represent the undrained shear strength.

Analysis of Pore Pressure Response

Of the 29 piezometers installed for the project, 18 were located in the vicinity of the three sections. Five piezometers were located at or beyond the toe of the embankment and these registered zero excess hydrostatic porepressure. As the tips of these piezometers were located near either El. 610 ft or 560 ft (186 m or 171 m), the measurements suggest that there was little spreading of excess hydrostatic pore-water pressure through horizontal layers of pervious soil.

Nine piezometers were located beneath the embankment and registered significant excess-hydrostatic pore pressures. Out of these, five had their tips located near El. 560 ft (171 m) which is the elevation of the lower soft layer. The pore pressures measured in these piezometers were compared with pore pressures estimated by available theories. For this purpose, the measured piezometric levels were plotted versus the embankment elevation as shown in Figs. 13(*a*) and 13(*b*). The solid lines show the rise in the piezometric level with loading and in a few cases a subsequent drop caused by consolidation. For example, the drops in piezometric level in Piezometer 11-70 when the embankment was at El. 640 ft and 648 ft (195 m and 198 m) occurred while no material was being added to the embankment (Fig. 6). To obtain the "undrained pore pressure" it was assumed that no consolidation took place during loading. The drop in pore pressure following loading was ignored and the pore pressure increments during the succeeding load increments were added together. The results are shown by the dashed lines in Figs. 13(*a*) and 13(*b*). Since some dissipation of pore pressure undoubtedly occurred during construction, this method underestimates the undrained pore pressure. The irregular shape of the curves is believed to indicate pore pressure response to stresses caused by embankment construction in areas adjacent to the piezometers. Because of the irregular construction pattern, it is not always possible to determine accurately the loading conditions at all times.

The high phreatic surface [Fig. 2, 3, 4, and 13(*b*)] is unusual and deserves attention. The phreatic surface was determined by observation of water levels in the slope indicator tubes. The space around each tube was packed with sand and was not sealed at the surface because of embankment construction. Thus, considerable surface water could have entered the tube. In our judgment the water levels are not representative of the phreatic surface. Therefore, the excess-hydrostatic pore pressure was taken to be the difference between the initial ground-water level and the piezometric level.

Piezometer 1 [Fig. 13(*a*)] showed a comparatively regular relationship between embankment elevation and piezometric level. The values of the undrained pore pressure, Δu, are plotted versus the principal stress, $\Delta\sigma_1$, for different stages of embankment construction in Fig. 14. For the other piezometers, only the

final pore pressure and final $\Delta\sigma_1$ are shown. Dashed line A represents the average behavior of these piezometers.

The pore pressure change, Δu, was estimated by the following methods. In

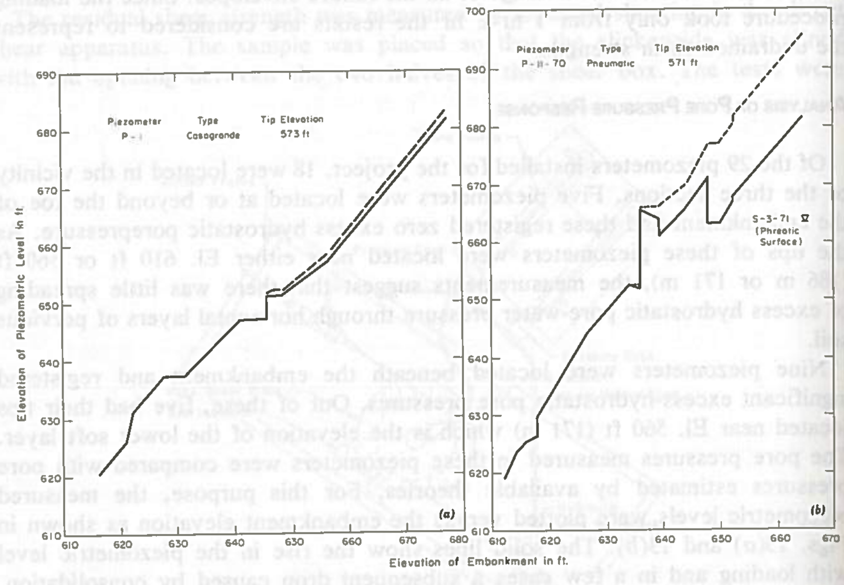

FIG. 13.—Piezometric Level Versus Embankment Height: (a) Piezometer P-1; (b) Piezometer P-11-70 (1 ft = 0.305 m)

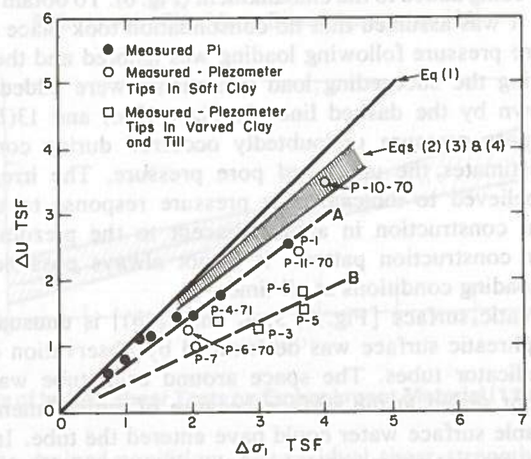

FIG. 14.—Comparison Between Computed and Measured Pore Pressures

the one-dimensional theory

$$\Delta u = \Delta\sigma_v \quad (1)$$

in which $\Delta\sigma_v$ = the change in vertical stress. In the elastic theory

$$\Delta u = \frac{1}{3}(\Delta\sigma_1 + \Delta\sigma_2 + \Delta\sigma_3) \quad (2)$$

in which $\Delta\sigma_1, \Delta\sigma_2, \Delta\sigma_3$ = the three principal stresses. In Skempton's theory (12)

$$\Delta u = \Delta\sigma_3 + A(\Delta\sigma_1 - \Delta\sigma_3) \quad (3)$$

and in Henkel's theory (4)

$$\Delta u = \Delta\sigma_{OCT} + \alpha\Delta\tau_{OCT} \quad (4)$$

in which σ_{OCT} and τ_{OCT} = octahedral normal and shear stresses, respectively. If the pore pressure is measured by triaxial tests, then

$$\alpha = \frac{3A - 1}{\sqrt{2}} \quad (5)$$

The stresses were computed by the finite element method for linear elasticity and for nonlinear elasticity. The values of A were taken from Fig. 3. As it turns out, the pore pressures computed by the elastic, Skempton's, and Henkel's theories are very close to each other. They are shown in Fig. 14 as a shaded zone. In general, the calculated pore pressures are slightly higher than the pore pressures measured in the silty clay as represented by line A. Note that if the phreatic surface is represented by the water levels in the slope indicator tubes, the measured pore pressure would be considerably less than the predicted values.

The changes in pore pressure measured by four piezometers whose tips were located in varved clay and glacial till are plotted in Fig. 14 as line B. The pore pressures are considerably smaller than those measured by piezometers located in the silty clay. The measured preconsolidation pressures of the varved clay and glacial till vary over a wide range. Thus, no attempt was made to predict the pore pressure from theory.

Stability Analysis

The stability of the embankment was analyzed by the method of Morgenstern and Price (11) using the observed failure surface. A total stress analysis was made assuming that the loading takes place in the undrained condition. Three methods may be used to choose the shear strength. The first method is to use one-half the unconfined compressive strength. The shear strengths for the various soils are shown in Table 1 and 2. A second method is to use the normalized shear strength from the simple shear test for the strength of the soft silty clay layer at El. 610 ft and 560 ft (186 m and 171 m), as shown in Tables 1 and 2. A third method is to use the normalized shear strength from the triaxial tests for the strength of the soft silty clay layer.

The computed safety factors for the three sections are given in Table 3. It can be seen that use of the shear strength from unconfined compression tests overestimates the safety factor for Sections AA and BB. Safety factors of 1.08 and 1.28 were obtained with the shear strength from simple shear tests. Note that the simple shear tests were performed on block samples taken from

a limited area. Unconfined compression tests indicate that the strengths of the block samples are somewhat higher than the average strength of tube samples taken from the failure zone. If this difference is not attributed to greater sampling disturbance sufferred by the tube samples then the average strength of the material in the failure zone may be less than the strength of the block samples used for simple shear tests. In view of this reservation, the computed safety factors of 1.08 and 1.28 are considered reasonable. Use of the triaxial test results leads to serious errors on the unsafe side.

TABLE 3.—Computed Safety Factors

Case (1)	Measuremant of shaar strangth (2)	Method of analysis (3)	Safety Factor		
			Section A-A (4)	Section B-B (5)	Section C-C (6)
1	Consolidate-undrained triaxial test	Effective stress	1.55	1.95	2.31
2	Simple shear test	Effective stress	1.13	1.46	1.70
3	Unconfined compression test	Total stress	1.25	1.44	1.57
4	Consolidated-undrained triaxial test	Total stress	2.91	1.73	2.68
5	Constant volume simple shear test	Total stress	1.28	1.08	1.69

TABLE 4.—Effect of Various Parameters on Safety Factor

Case (1)	Method of analysis (2)	Maasuramant of strength (3)	Paramater studied (4)	Section (5)	Safety factor (6)
1	Total stress	Simple shear	p_c = 3.0 tsf	A-A	1.19
				B-B	1.04
2	Total stress	Simple shear	p_c = 4.0 tsf	A-A	1.44
				B-B	1.10
3	Total stress	In-situ shear test on fill	c_u = 0.4 tsf ϕ_u = 11.5°	A-A	1.29
				B-B	1.38
4	Effective stress	Simple shear	Reduced pore pressure	A-A	1.43
				B-B	2.00
5	Effective stress	Simple shear	High pore pressure	A-A	1.00
				B-B	1.38

Note: 1 tsf = 95.8 kN/m².

Effective stress analyses were made using $\bar{c}$ and $\bar{\phi}$. The shear strength parameters used are given in Tables 1 and 2. At Section CC several piezometers had their tips near El. 565 ft (172 m) and the piezometric surface as shown in Fig. 4 was used to determine the pore pressure. At Sections AA and BB none of the piezometers had their tips near the elevation of the slip surface. Thus, the piezometric surface was estimated from the relationship shown as curve A in Fig. 14. Note that this is the estimated pore pressure for the undrained condition in the silty clay. The pore pressures in the varved clay and till should

be smaller. Thus, the analyses may underestimate the safety factor. However, the computed safety factors are all considerably larger than 1. Therefore analyses with the results from both the simple shear and triaxial tests lead to overestimates of the safety factor.

The preceding safety factors were obtained with mean values of shear strength and judgment was involved in the choice of the preconsolidation pressure and the pore pressure. Therefore, it is desirable to investigate the effects of these parameters on the computed safety factor.

In the total stress analysis the evaluation of the shear strength from the results of simple shear tests is based on a preconsolidation pressure of 3.5 tsf (340 kN/m²). It may be as low as 3.0 tsf (290 kN/m²) or as high as 4.0 tsf (380 kN/m²). The safety factors obtained with these values are given in Table 4 as Cases 1 and 2. As another possibility, we may choose to use the results of the in-situ shear tests to represent the strength of the fill. Then c_u = 800 psf (38 kN/m²) and ϕ_u = 11.5°. With other conditions remaining the same as for Case 5 in Table 3, a safety factor of 1.38 was obtained for Section BB (Case 3 in Table 4). The safety factor for Section AA does not change appreciably.

In effective stress analysis, a major uncertainty is the pore pressure at failure. The effect of the pore pressure on the safety factor was investigated by stability analyses in which the pore pressures in the varved clay and till were taken as one-half of those determined from the piezometric levels shown in Figs. 2 and 3. This is considered to be a more realistic estimate of the pore pressure in the varved clay and till. The computed safety factors for this reduced pore pressure are given in Table 4 as Case 4. On the other hand, field measurements have shown that the pore pressures after failure may be much larger than those before failure (6). For Case 2 in Table 3, the pore pressure is represented by line A (Fig. 14). If the pore pressure in the failure zone increased during failure, the pore pressure after failure could have been higher than that represented by line A. For this reason, stability analyses were made with piezometric levels that are 10 ft (3.3 m) above those shown in Figs. 2 and 3 over the top of the embankment. The piezometric levels then drop at a uniform rate to coincide with the piezometric levels in Figs. 2 and 3 at the toe of the embankment. The computed safety factors are given in Table 4 as Case 5.

Finally for Case 1 in Table 3, if we use $\bar{\phi}$ = 27.5° for the silty clay and $\bar{\phi}$ = 35° for the fill as suggested by lines A and B in Fig. 8, slightly different safety factors would result. However, the changes in the safety factors are insignificant.

Uncertainty

The results of stability analyses have shown that the computed safety factor may vary over a considerable range although the inputs may all be considered "reasonable." Thus, it is desirable to evaluate the uncertainties.

It may be asked first whether the failure should have been expected if all the information had been available prior to construction. Alternatively, using the computed safety factors and the observed performance, deductions may be made on the reliability of the methods used for determination of shear strength. The average of the safety factors for Sections AA and BB is taken to represent

that of the slide. Accepting the proposition that the simple shear test gives the best measure of the undrained shear strength, the safety factor of 1.18, which is the average of 1.28 and 1.08 (Case 5 in Table 3), represents the best answer according to our judgment. Due to uncertainties in the preconsolidation pressure the safety factor may range from 1.12–1.27 (Cases 1 and 2 in Table 4). If it is assumed that the safety factor is a random variable with a uniform distribution between these limits, the coefficient of variation, V_1 is 0.07.

Other sources of uncertainty that should be considered include soil variability, progressive failure, strain-rate effect, and inaccuracies in stability analysis. To evaluate soil variability we note that the coefficient of variation of the undrained shear strength as measured by the unconfined compression test for both varved clay and silty clay is approx 0.5. Using the spatial correlation developed in Ref. 13 leads to a coefficient of variation of the order of $V_2 = 0.2\ V_s$ for the average shear strength along the slip surface, in which V_s denotes the coefficient of variation of the test results. This assumes that the slip surface is approximately circular and passes through a series of layers. If a significant portion of the slip surface follows a weak layer V_2 would be larger and of the order of $0.4\ V_s$. Using the latter case, we obtain $V_2 = 0.20$. The errors due to progressive failure, strain-rate effect, and inaccuracies in analysis cannot be determined precisely, but estimates based on published information have been made (14,15). These estimates indicate that the sum of these effects would change the safety factor by −5% to +15% and the coefficient of variation is between 0.10 and 0.17. In the following calculations it is assumed that the net effect on the safety factor is zero and the coefficient of variation, V_3, is 0.15.

Using the approximation that

$$V^2 = V_1^2 + V_2^2 + V_3^2 \quad \ldots\ldots\ldots\ldots\ldots\ldots\ldots\ldots\ldots\ldots\ldots\ldots\ldots\ldots (6)$$

in which V = the coefficient of variation of the safety factor, $V = 0.26$ is obtained for total stress analysis with the shear strength as determined by the simple shear test. For a safety factor of 1.18, the failure probability is of the order of 0.27. Thus, failure should be considered as likely. If a low failure probability of, say, 10^{-2} (10,14) is required, the safety factor should be about 1.70. Note that this is close to the computed safety factor for section CC (Case 5 in Table 3). We next consider the computed safety factors with the knowledge that failure has occurred. The probability that the difference between the computed safety factor and the observed safety factor of 1.0 is due to the random errors described previously is 0.27, whereas the probability that the difference is due to an incorrect evaluation of the shear strength is 0.73; the latter is more likely. Thus, we conclude that for this particular case history the safety factor obtained should be corrected by −16% and the uncertainty may be represented by a coefficient of variation of about 0.26.

As an alternative, we may also consider the strength of the fill as a source of uncertainty. Then the safety factor is 1.34, which is the average for Case 3 in Table 4, may be taken as the upper limit; the lower limit is still 1.12, (Case 1 in Table 4). If we choose the average of 1.23 as the best answer, $V_1 = 0.18$. The calculated failure probability is not significantly different from that in the preceding case.

A similar analysis can be made for the effective stress analysis with $\bar{c}$ and $\bar{\phi}$ as measured by the simple shear test. In our judgment, the conditions for Case 2 in Table 3 represent the best estimate of the in-situ conditions and the safety factors given for Case 5 in Table 4 are considered to be the lower limit. The safety factors computed with the reduced pore pressure, (Case 4, Table 4) are considered to be the most optimistic estimate. Again assuming a uniform distribution between these limits, the coefficient of variation, V_1, is 0.19 and represents the uncertainty in the pore pressure. The soil variability as reflected by the scatter in $\bar{\phi}$ from triaxial tests is represented by a coefficient of variation, $V_2 = 0.11$. The value of V_3 is taken to be 0.15 as before. Eq. 6 then gives $V = 0.27$ for the safety factor and the failure probability is of the order of 0.23. Thus, failure should also be considered likely. The probability that the difference between the computed and observed safety factors is due to an incorrect evaluation of the shear strength is 0.77.

Summary and Conclusions

Failure of an embankment occurred along a slip surface whose major portion followed a relatively thin layer of soft clay. The measured deformations and pore pressures are summarized. Stability analyses using the undrained shear strength as measured by the simple shear test gave safety factors that are of the right order of magnitude. Safety factors obtained with results of unconfined compression tests and triaxial tests are still larger. Stability analyses with effective stress and using the shear strength from simple shear and triaxial tests also overestimate the safety factor.

Probability analysis was used to evaluate the effect of the various uncertainties on the computed safety factors. It was concluded that discrepancies between computed and observed safety factors are most likely the result of errors in the estimation of shear strength. This conclusion is of course based on our choice of best estimates and upper and lower limits, as well as our judgment of uncertainties introduced by variation in soil properties and accuracy of analysis.

Acknowledgment

This investigation was sponsored by the Ohio Department of Transportation and the Federal Highway Administration. The opinions expressed in this paper are those of the writers and do not necessarily reflect the views of the sponsors. We are grateful to R. Bashore, R. O. Calvin, H. E. Marshall, and C. H. Shephard, all of the Ohio Department of Transportation, for their collaboration in the field measurements, to T. Y. H. Chang and A. El-Refai for assistance in the laboratory work, and to N. R. Morgenstern for making available his computer program. The original manuscript was revised extensively following consideration of the criticisms and suggestions by an ASCE reviewer. His contributions are greatly appreciated.

Appendix I.—References

1. Bagley, C. T., "Subsurface Study of Glacial Deposits at Cleveland, Ohio (abstract)," *Geological Society of America Bulletin*, Vol. 61, 1950, pp. 1561–1562.
2. Bjerrum, L., and Landva, A., "Direct Simple Shear Tests on Norwegian Quick Clay,"

Geotechnique, London, England, Vol. 16, 1966, p. 1.
3. Cushing, H. P., Leverett, F., and van Horn, F. R., "Geology and Mineral Resources of the Cleveland District, Ohio," *U.S. Geological Survey Bulletin 818*, 1931.
4. Henkel, D. J., and Wade, N. H., "Plane Strain Tests on a Saturated Remolded Clay," *Journal of the Soil Mechanics and Foundations Division*, ASCE, Vol. 92, No. SM6, Proc. Paper 4970, Nov., 1966, pp. 67–80.
5. Hirst, T. J., and Mitchell, J. K., "Compositional and Environmental Influences on the Stress-Strain-Time Behavior of Soils," *Report TE 68-4*, Department of Civil Engineering, University of California, Berkeley, Calif., 1969.
6. Ladd, C. C., "Test Embankment on Sensitive Clay," *Proceedings of the ASCE Specialty Conference on Earth and Earth Supported Structures*, Vol. 1, 1972, p. 101.
7. Ladd, C. C., Aldrich, H. P., and Johnson, E. G., "Embankment Failure on Organic Clay," *Proceedings of the 7th International Conference on Soil Mechanics and Foundation Engineering*, Vol. 2, 1969, p. 627.
8. Ladd, C. C., and Foott, R., "New Design Procedure for Stability of Soft Clays," *Journal of the Geotechnical Engineering Division*, ASCE, Vol. 100, No. GT7, Proc. Paper 10664, July, 1974, pp. 763–786.
9. "Large Torsion Shear Tests, Alternate 5A, Embankment Stability, I-77/I-480 Interchange, Independence, Ohio," Shannon and Wilson, Inc., Seattle, Wash., 1972.
10. Meyerhoff, G. G., "Safety Factors in Soil Mechanics," *Canadian Geotechnical Journal*, Vol. 7, 1970, p. 349.
11. Morgenstern, N. R., and Price, V. E., "The Analysis of the Stability of General Slip Surface," *Geotechnique*, London, England, Vol. 20, 1965, p. 79.
12. Skempton, A. W., "The Pore pressure Coefficients A and B," *Geotechnique*, London, England, Vol. 4, 1954, p. 148.
13. Wu, T. H., "Uncertainty Safety and Decision in Soil Engineering," *Journal of the Geotechnical Engineering Division*, ASCE, Vol. 100, No. GT3, Proc. Paper 10434, Mar., 1974, pp. 329–348.
14. Wu, T. H., and Kraft, L. M., "Safety Analysis of Slopes," *Journal of the Soil Mechanics and Foundations Division*, ASCE, Vol. 96, No. SM2, Proc. Paper 7174, Mar., 1970, pp. 609–630.
15. Yuceman, M. S., Tang, W. H., and Ang, A. H. S., "A Probabilistic Study of Safety and Design of Earth Slopes," *Structural Research Series No. 402*, Civil Engineering Studies, University of Illinois, Urbana, Ill., 1973.

Appendix II.—Notation

The following symbols are used in this paper:

A = pore pressure parameter;
$\bar{c}$ = cohesion;
p_c = preconsolidation pressure;
s_u = undrained shear strength;
u = pore pressure;
V_i = variance;
σ_{oct} = octahedral normal stress;
σ_{vm} = maximum past pressure;
σ_y = vertical stress;
$\sigma_1, \sigma_2, \sigma_3$ = principal stresses;
τ_{oct} = octahedral shear stress; and
ϕ = angle of internal friction.

JOURNAL OF THE GEOTECHNICAL ENGINEERING DIVISION

A Case History of Expansive Claystone Damage

By Richard L. Meehan,[1] M. ASCE, Michael T. Dukes,[2] and Patrick O. Shires[3]

Introduction

In the mid 1960's urban development was initiated in an extensive area of hilly terrain located in the western portion of the City of Menlo Park, Calif., 25 miles south of San Francisco. The development consisted of a residential community consisting of a mix of $75,000 custom-built houses on half-acre lots, clustered apartment and townhouse units, and professional office buildings, interfingered with a first class 18 hole golf course. By 1970, the project was well underway, with 300 houses and 700 apartment units constructed and sold, 17 miles of residential streets completed, and planning for the complete development of the remainder of the open land actively underway.

It was at about this time that distressing signs of unusual ground behavior began to surface, at first in the form of minor movement of house foundations and cracking and heaving of street pavements. Ground stability had become a matter of momentary but serious concern in 1966, when a 1-acre landslide developed on relatively gently sloping ground, affecting three lots and partially destroying one house, but this easily diagnosed slide failure had happily proved to be an isolated event. However, by 1970, the continued damage to houses due to expansion or downhill creep of clay-rich shales or their soil products, leading in several instances to major cracking of strip footings and other masonry, tilting and warping of building frames, and destruction of some swimming pools, continued to escalate at a rate that was alarming to property owners, the developer, and city officials.

Note.—Discussion open until February 1, 1976. To extend the closing date one month, a written request must be filed with the Editor of Technical Publications, ASCE. This paper is part of the copyrighted Journal of the Geotechnical Engineering Division, Proceedings of the American Society of Civil Engineers, Vol. 101, No. GT9, September, 1975. Manuscript was submitted for review for possible publication on November 26, 1974.

[1]President, Earth Sciences Assocs., Palo Alto, Calif.
[2]Staff Engr., Earth Sciences Assocs., Palo Alto, Calif.
[3]Staff Engr., Earth Sciences Assocs., Palo Alto, Calif.